

A Two-Dimensional, Semiconducting Bolometer Array for HAWC

George M. Voellmer^{*a}, Christine A. Allen^a, Sachidananda R. Babu^a; Arlin E. Bartels^a,
C. Darren Dowell^b; Jessie Dotson^c; D. Al Harper^d; S. Harvey Moseley^a; Timothy Rennick^d;
Peter Shirron^a; W. Wayne Smith^e; Edward J. Wollack^a

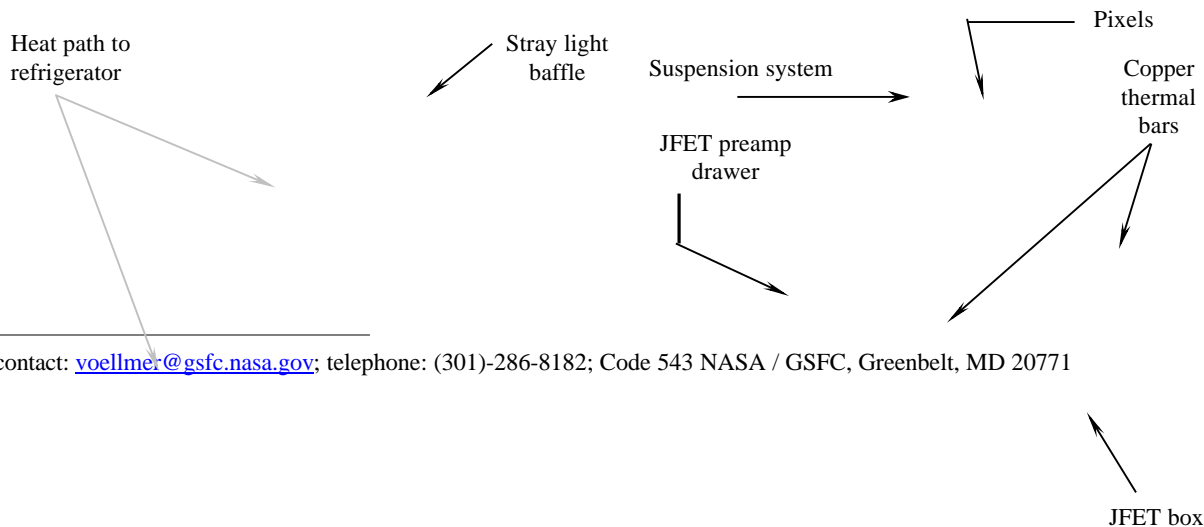
^aNASA Goddard Space Flight Center; ^bCaltech/JPL; ^cNASA Ames Research Center; ^dUniversity of Chicago; ^eOSC/GSFC

ABSTRACT

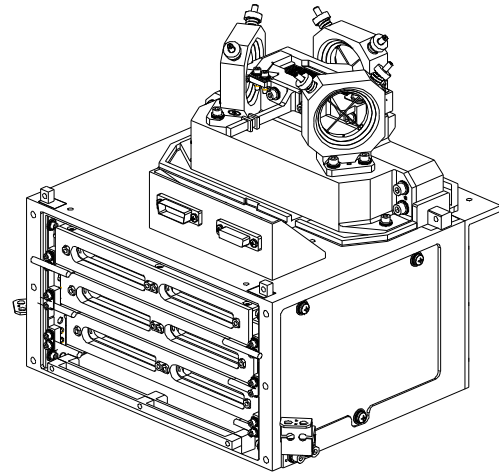
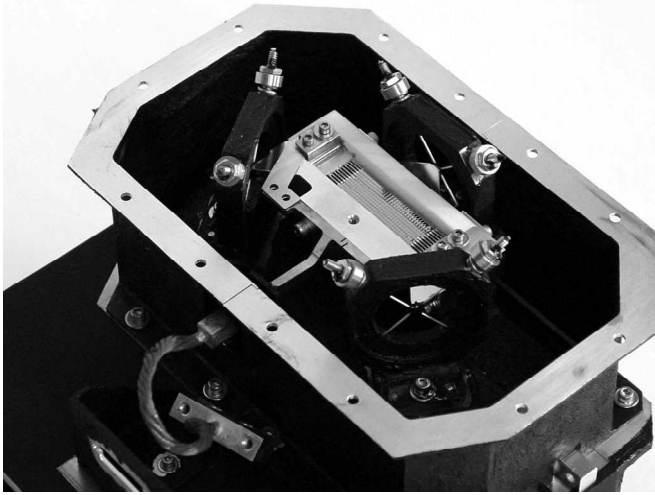
The Stratospheric Observatory For Infrared Astronomy's (SOFIA's) High resolution Airborne Wideband Camera (HAWC) will use an ion-implanted silicon bolometer array developed at NASA's Goddard Space Flight Center (GSFC). The GSFC Pop-Up Detectors (PUDs) use a unique "folding" technique to enable a 12 x 32 element close-packed array of bolometers with a filling factor greater than 95%. The HAWC detector uses a resistive metal film on silicon to provide frequency independent, ~50% absorption over the 40 – 300 micron band. The silicon bolometers are manufactured in 32-element rows within silicon frames using Micro Electro Mechanical Systems (MEMS) silicon etching techniques. The frames are then cut, "folded", and glued onto a metallized, ceramic, thermal bus "bar". Optical alignment using micrometer jigs ensures their uniformity and correct placement. The rows are then stacked side-by-side to create the final 12 x 32 element array. A kinematic Kevlar suspension system isolates the 200 mK bolometer cold stage from the rest of the 4K detector housing. GSFC – developed silicon bridge chips make electrical connection to the bolometers, while maintaining thermal isolation. The Junction Field Effect Transistor (JFET) preamplifiers for all the signal channels operate at 120 K, yet they are electrically connected and located in close proximity to the bolometers. The JFET module design provides sufficient thermal isolation and heat sinking for these, so that their heat is not detected by the bolometers. Preliminary engineering results from the flight detector dark test run are expected to be available in July 2004. This paper describes the array assembly and mechanical and thermal design of the HAWC detector and the JFET module.

1. INTRODUCTION

HAWC [1] is a far-infrared instrument being built to study star formation, protoplanetary disks, and interstellar gas and dust. HAWC will be a facility instrument for the Stratospheric Observatory for Infrared Astronomy, an airborne telescope housed in a converted Boeing 747SP. It will use a 384-element bolometer array developed at the GSFC (Figs. 1&2). An almost identical engineering unit of the HAWC detector has been in use at the Caltech Submillimeter Observatory since July 2002 as part of the Submillimeter High Angular Resolution Camera (SHARC) II instrument [2].



*contact: voellme@gssc.nasa.gov; telephone: (301)-286-8182; Code 543 NASA / GSFC, Greenbelt, MD 20771



Figs. 1&2: The HAWC detector

2. DETECTOR MECHANICAL DESIGN

Bolometer Absorber

The heart of the detector is the bolometer absorber. The absorber captures incident infrared radiation and translates it into thermal energy, resulting in a temperature rise in the bolometer element. The change in temperature is measured with a temperature-dependent, ion-implanted resistor, also located on the body of the bolometer. The absorber is thermally evaporated directly on the back side of the detector body, to provide good thermal coupling, without electrically shorting out the implanted resistor on the front-side. The absorber, a resistive metal film of titanium gold with broad absorptivity, is used to couple to the incoming radiation over the 40 -300 μm waveband. A target resistance of 157 Ω per square on a silicon substrate results in frequency independent coupling (within this waveband) to the incident radiation field. With this impedance level, $\sim 30\%$ the power is reflected from the structure, half of the light is absorbed in the thin film metallization, and the remainder is transmitted. The transmitted power is in turn absorbed by a layer of epoxy loaded with glass beads residing behind the absorber structure. The deposited metal films are relatively thin and as a disordered metal system, the surface resistivity does not change appreciably in cooling. In practice, the ~ 1 micron silicon membrane thickness in use is relatively electrically thin and relaxes the resistivity requirement to achieve frequency independent absorption over the band. Best results were obtained with a target resistance of $\sim 120 \Omega$ per square.

2.1 PUD array folding

The most unique feature of these detectors is the “folding” of the semiconductor bolometers [3]. This is the key innovation which enables an absorber to abut its neighbors on all four sides with only a few percent of the collecting area unfilled.

More detail about the bolometer fabrication can be found in [4], but briefly, the PUDs (Fig. 3) are manufactured in 32-element, planar rows using MEMS semiconductor etching techniques. Instead of the more typical, straight legs attaching the absorber to the frame, PUDs have a torsional yoke attachment, visible in Figure 5. When the frame of the bolometer is cut as shown in Figure 4, and the two sides of the frame are folded together, the torsional section twists and allows the legs to fold under the absorber, forming a table-like structure (Fig. 4). This allows adjacent rows to be packaged very closely together (Fig. 5).

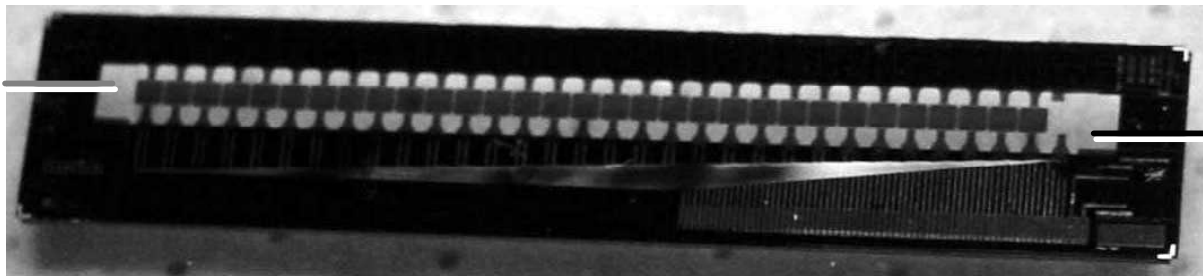


Figure 3: Unfolded PUD array showing frame cut lines.

Torsional yoke attachment

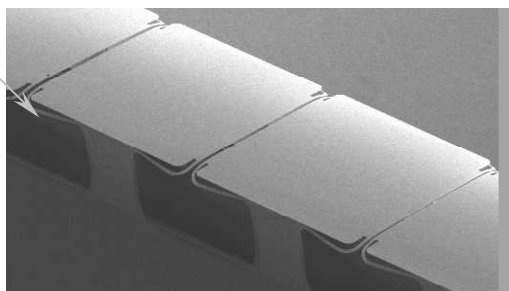


Figure 4: Folded PUD array

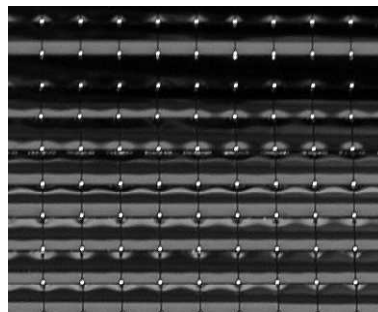


Figure 5: Close-packed 2-D array of folded PUDs – the HAWC array (seen face-on).

The frame halves are glued to a copper and gold plated, ceramic, thermal bus bar with a very thin ($<25\mu\text{m}$ (.001")) film of Epon 815C resin and Versamid 140 hardener, mixed 3:2 [5], providing good thermal and mechanical connection to the thermal sink. Manual alignment during the two-step gluing operation, using specialized jigs (Figs.6&7) under a microscope, ensures a given row's uniformity and correct placement with respect to the reference edge of the bus bar. The finished bus bar /PUD assemblies are then butted up and glued against reference surfaces in a ceramic frame, called the "upper C" because of its shape, which aligns all the pixels to each other.

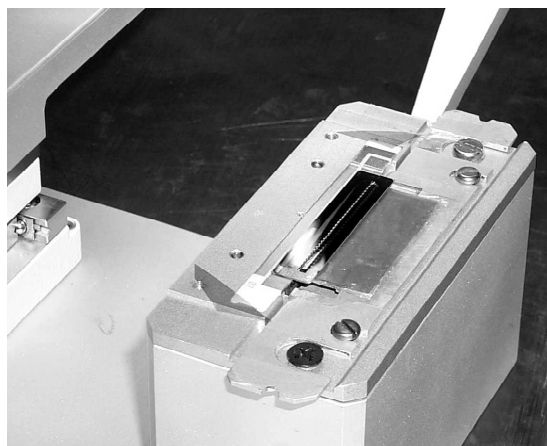


Figure 6: Unfolded PUD in folding jig.

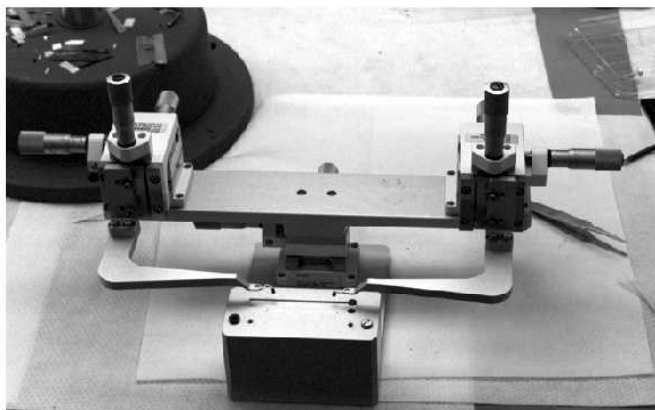


Fig. 7: PUD Alignment Jig

Immediately beneath the bolometer absorber, the top edge of the bus bar widens out to almost the same size as the absorber (Fig. 8). As the HAWC detector is a broadband instrument, covering wavelengths from 40 - 300 μm , a single resonant cavity behind the absorber would not absorb evenly over the entire wavelength range, and was hence to be avoided. This top edge was therefore coated with a mixture of the Epon / Versamid epoxy, carbon black (47% by weight Epon, 47% Versamid, 6% Carbon black). Glass beads sifted down to $<40 \mu\text{m}$ were then applied to the wet glue (Fig. 9).

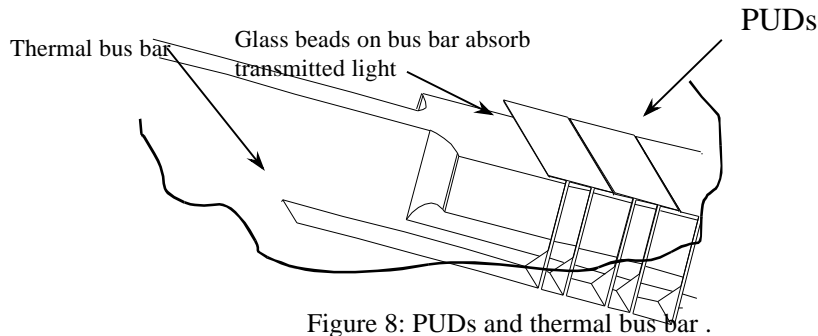


Figure 8: PUDs and thermal bus bar .

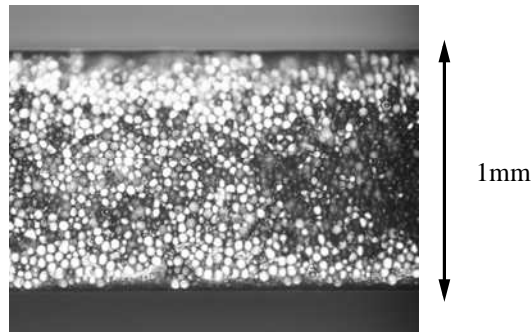


Figure 9: Close-up of glass beads on Bus Bar edge

2.2 Fanning out the signals

In the finished detector, the PUD/bus bar assemblies will be stacked one next to the other. The center-to-center pitch of the pixels was set at 1000 μm . This pitch was chosen as the best compromise between the competing constraints of final detector array size, required optics focal lengths for Nyquist sampling, and feasibility of packaging. The bolometer's absorber area was made slightly smaller than the pixel pitch, to allow for small variations in the folding. The pixel pitch sets the scale of the mechanical package: all the mechanical support and electrical connections for a given PUD row had to fit completely behind that row. The rows and their respective connections are then stacked up to build up the two-dimensional array.

The stacking arrangement is shown in Fig. 10. Alumina ceramic was chosen as the bus bar material because of its close thermal expansion match to the silicon PUDs that are glued to it. To have adequate strength, the bus bar needed to be at least .25 mm (.010") thick. For heat sinking the bolometer frames, .05 mm (.002") thick copper plating was used on both contact surfaces of the bus bar. A thin flash of gold inhibits corrosion and improves the thermal contact. The silicon frames themselves are .30 mm (.012") thick, and we allowed for .038 mm (.0015") thick glue lines. A

minimum of .38 mm (.015") vertical clearance is required to accommodate the wirebonds that electrically connect the bolometers to the outside world.

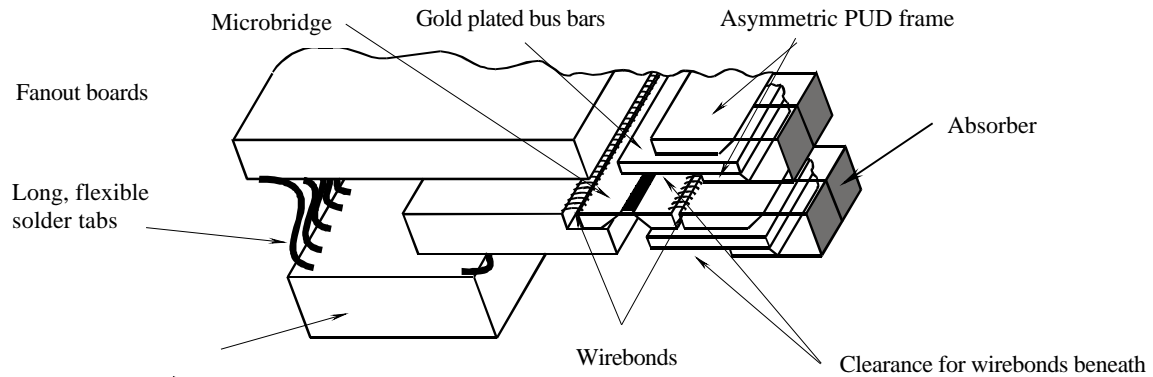


Figure 10: Stacking arrangement.

To help accommodate the wirebonds, the PUD frames are asymmetric, as can be seen in Figures 3&10. When the sides of the frame are cut and it is folded over a bus bar, the side with the wire bond pads extends further than the side without them. Thus, when the next row is laid on top, a small additional space is left above the wirebond pads.

2.3 Detector core assembly

The bolometer assemblies are glued into a ceramic holder, the “upper C”. When the detector is complete, a Kevlar suspension system mechanically connects the bolometers to the main detector structure. The bolometer assemblies glued into the upper C comprise the part of the detector which is to be cooled to 200 mK, and which thus needs to be thermally isolated from the rest of the detector. During the buildup, however, temporary alignment bars maintain proper positioning between the upper C and the strongback (Fig. 11). A PUD/bus bar assembly, prepared as described in the previous section, is glued into the ceramic upper C using Epon/Versamid. One ceramic fanout board is glued into the titanium strongback for each row of PUDs. Silicon microbridges [6](Figs. 10&12) are used to make electrical contact between the cold PUDs and the warmer fanout boards with a minimum of thermal conduction. A microbridge chip is glued in position to interconnect the PUD and the fanout board, the wirebonds are made, and the frame of the microbridge chip is laser cut, completing the thermal isolation.

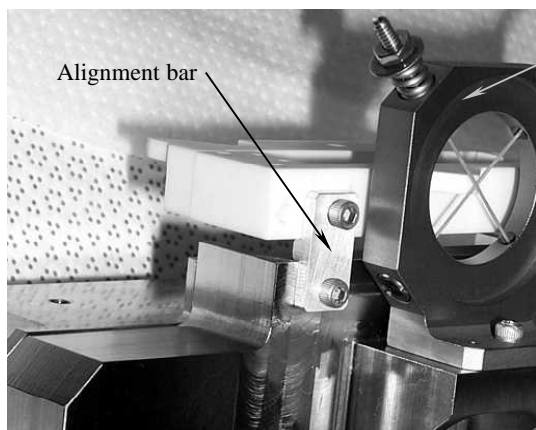


Figure 11: Temporary alignment bars hold the cold stage in position prior to suspension system gluing

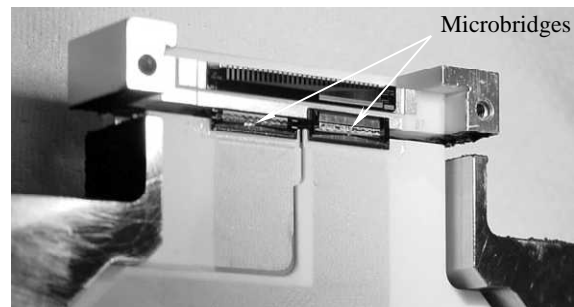


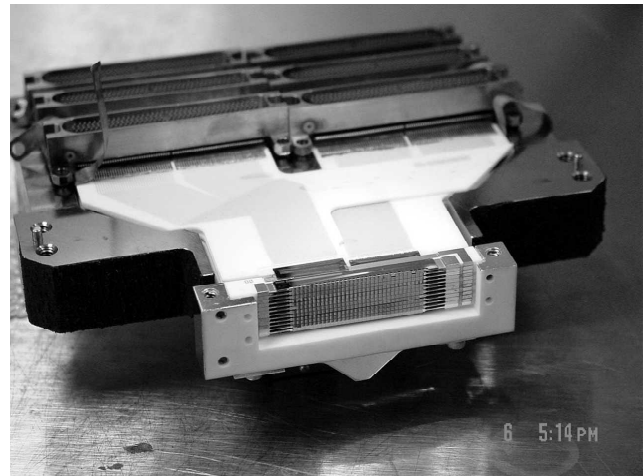
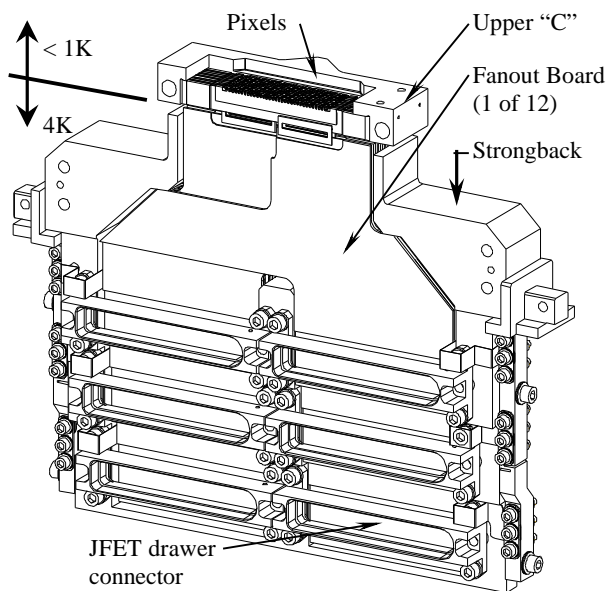
Figure 12: The electrical connections are made across temperature stages using microbridges. Connections are staggered left and right on successive layers.

As the rows of PUDs are stacked up, corresponding bond pads on the PUDs and on the fanout boards, as well as the microbridges which interconnect them, are staggered left and right on successive layers to give more headroom for the wirebonds on the fanout boards (Fig. 12). By leaving room in this way, the fanout boards could be made thicker and stronger. The fanout boards are also alumina, for a good CTE match to the bridge chips which are glued to them.

The lower end of the fanout boards is where the connectors are soldered in place. The detector has 12 bolometer rows and three JFET drawers, so each connector has to make contact with four fanout boards. As the fanout boards are each behind its own PUD row, they are at 4 different heights, 1 mm apart. Large, dense connectors from Packard-Hughes (now Delphi Connection Systems)[7] were used with long, flexible solder contacts, which were bent to reach the different levels of the fanout boards (Figs. 10&14). These connectors are anchored to the strongback to prevent mating forces from bending the solder leads.

The core of the detector (Figs. 13&14) consists of this stack of 12 ceramic printed circuit boards, or “fanout boards”, each with a folded, 32-element, linear PUD bolometer array arranged on one edge, and a JFET “drawer” extending orthogonally from one face.

Structurally, the fanout boards are glued into a titanium strongback: titanium was chosen because its integrated CTE is sufficiently close to that of alumina to permit this style of attachment.



Figures 13&14: Detector core (without JFET drawers or suspension system).

2.4 Thermal isolation system

The bulk of the detector operates at 4K. Two thermal isolation systems were required for this detector: between the bolometer stage and the main structure, and between the JFET boards and the surrounding JFET drawer. The PUD bolometer assembly operates at 200 mK, which is why the Kevlar suspension is needed. The JFETs operate at 120K, only 15 cm (6”) away from the bolometers, so thermal isolation and radiation blocking are critical design features.

The base of the PUD bolometers needs to be kept at 200 mK. A very low thermal conductivity mount from this cold stage to the rest of the 4K detector is desirable for two reasons: to minimize the load on the cold stage refrigerators, and to isolate the PUD bases from fluctuations in the helium bath temperature. We chose to make a tensile structure out

of unbraided, 2160 denier, type 968, Kevlar 49 cord because of its low conductivity (2×10^{-4} W/cm·K at 4K) [8] and high stiffness (112 GPa @ room temp)[9]. The Kevlar cord is glued into fittings using Stycast 2850 with 24LV catalyst [10]. The lower fitting slides into a matching recess in the suspension tower (Fig. 11), which rigidly constrains the cord along its length. The Kevlar cord crosses the open part of the tower and the upper fitting protrudes from the top side of the tower, where a compression spring and nut are used to preload the cord (Figs. 1 & 11). Two cords are fitted to each of three towers in this fashion. The cold stage is glued at each of the three points where the cords cross, with a drop of Stycast.

An individual preloaded cord is stiff along its length (in both directions, as long as the preload is not exceeded), but relatively soft in the orthogonal directions. A pair of crossed cords in a tower is therefore stiff in the plane of the cords, but is soft normal to this plane and in all three rotation axes. Placing three of these Kevlar tower assemblies at roughly 120 degrees yields a kinematic attachment between the bolometer stage and the rest of the detector. This is desirable to prevent stress buildup, and to prevent lateral shifting of the center of the detector array, during cooldown. The three axes normal to the planes of the Kevlar cords in the three towers intersect at the center of the array, making that the temperature invariant point.

With the cold stage isolated in this fashion, the power from the 4 K stage to the 300 mK stage (as measured on the engineering unit) was only $4 \mu\text{W}$, feeding in from the Kevlar cords and the microbridges. The bus bars were connected to the 200 mK refrigerator as follows (Fig. 1): a copper foil was glued to the copper plating on the bus bar using the Epon/Versamid epoxy, mixing in 70 percent by weight silver powder, to make a conductive joint. The other end of the foil was clamped to a copper bar. This bar had features to form a labyrinth seal where it penetrated the stray light baffles (Fig. 1), which, while avoiding contact with the 4K baffle, prevented light from entering the PUD vicinity. A flexible copper braid for attachment to the refrigerator is silver brazed into a hole at the end of the bar. This clamps to the heat strap coming from the Adiabatic Demagnetization Refrigerator (ADR).

The JFETs (Figure 15) must be heated to 120 K to minimize their thermal voltage noise, and the total power dissipated (heaters plus JFET dissipation) should be at most on the order of 200 mW, to keep the helium boiloff for the instrument to 1 fill / day. The JFETs therefore are isolated on a 120 K “Warm Board” daughterboard within the 4K “Cold Board”. Thin walled Vespel tubes provide the mechanical support, and GSFC “Microbridge” chips provide the electrical connection. The approximately 400 microbridge interconnects to each JFET board conduct about 2 mW total from 120 K to 4.2 K, and radiative losses for each of the three JFET warm boards come to about 15 mW. A pair of 6.3 mm (.25”) long, 6.3 mm diameter Vespel® SP-1 tubes with a .13 mm (.004”) thick wall (Fig. 16) conduct approximately 14 mW, keeping the system well within the dissipation budget.

2.5 Radiation shielding and heat sinking

Good thermal isolation is half the battle in keeping the unwanted heat from the 120 K JFETs away from the bolometers: it reduces the power injected into the detector to heat the JFET warm board. Good thermal heat sinking and radiation blocking is equally important. Since a perfect seal cannot be accomplished, as the conductive traces will need to penetrate any seal, multiple stages of isolation, radiation blocking, and heat sinking are required.

The JFET drawer structure consists of the warm JFET board mounted to a ceramic cold board with Vespel tubes as described above, inside a titanium housing (Fig.15). Titanium was used because of its CTE match to the ceramic. The first line of defense against radiation from the JFET board is an opaque, conductive metal barrier around the warm JFET board. The top of this barrier is formed by a JFET board shield, and the bottom by the copper plating on the ceramic cold board. A labyrinth seal is made between the two by gluing a rectangular frame of gold plated ceramic to the cold board, which meshes with the shield. To avoid shorting out the traces on the cold board, the underside of this seal was not plated. Of course, this is a necessary radiation leak.

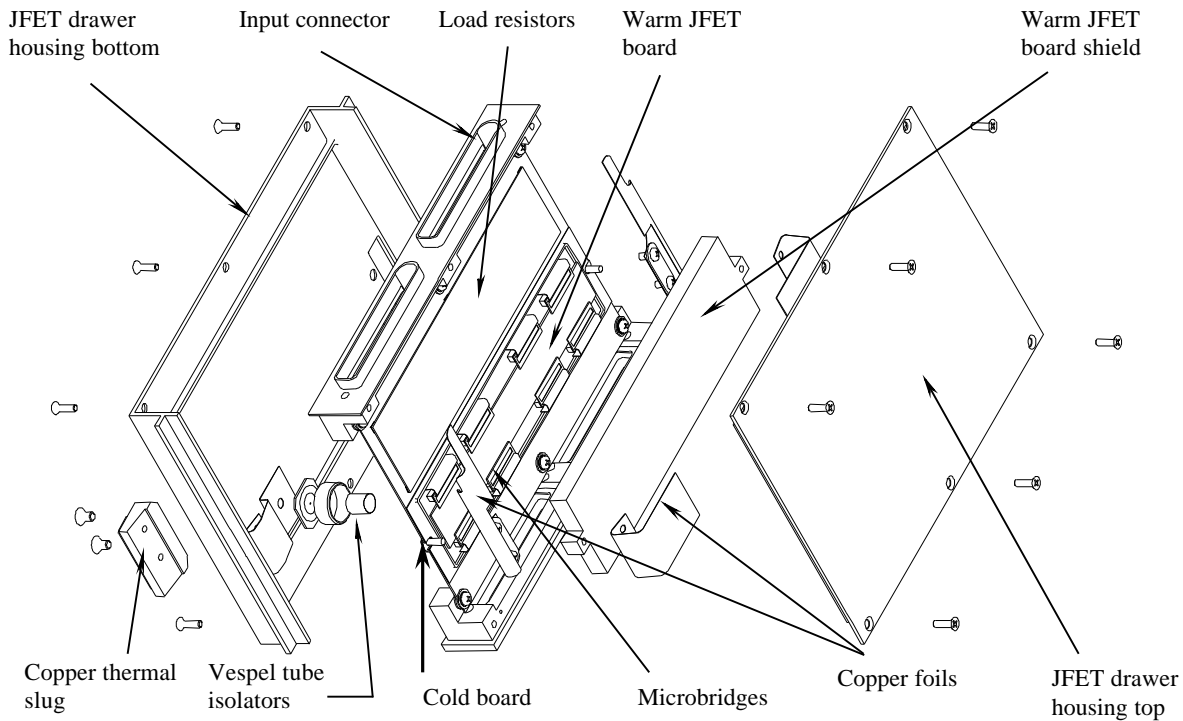


Figure 15: Exploded view of JFET drawer

The JFET Warm Board cover and the plating on the Cold Board are well anchored to the helium tank: the titanium housing for the JFET drawer, the second line of defense against JFET radiation, has a copper slug which penetrates through it. The slug provides a good thermal path through the shield, while keeping the enclosure light-tight. Copper foils, glued to the warm JFET board cover and to the plating on the cold board and then clamped to the inside of the slug, provide a conductive path. Copper ribbons are clamped to the outside of the slug, which are in turn clamped to copper thermal bars that penetrate the JFET box (Fig. 2), the third and final radiation barrier. At each radiation barrier penetration, the copper path serves to cool the barrier material. Where the copper thermal bars emerge from the JFET box, they are strapped to the helium tank using copper ribbons or braid.

At the connectors, the electrical traces penetrate the JFET drawer covers, creating a chink in the armor. To fortify this area, aluminized Mylar strips were inserted inside the solder tabs of the connector as a radiation barrier (the solder tabs are coated in this area, so shorting is not a problem), and the fanout boards had copper foils glued to their backs as a heat sink. Tabs on the foils were clamped to copper bars that penetrated the JFET box enclosure, which were in turn anchored to the helium tank. These foils ensured that the parts of the detector close to the bolometers were as cold as possible.

Finally, a last metal radiation baffle at the top of the fanout boards, with a stripe of absorptive epoxy [11] as “caulking”, absorbs most of the remaining radiation.

3. ENGINEERING RESULTS FROM SHARC II

The first light run of the SHARC II instrument in April 2002 presented an opportunity to verify the performance of the mechanical design. The primary concerns were: 1) How many pixels work? 2) How much will the power from the JFETs heat the bolometer frames? and, 3) How much will radiation from the JFETs heat the bolometer absorbers? Secondary concerns were: 4) Will the load resistors, inside the JFET drawers be heated above their 8K thermal noise threshold? 5) Will the fanout boards, carrying the high impedance signals from the PUD array, be susceptible to

microphonics? and, 6) How much power are the heaters using to warm the JFETs, and will they boil off too much helium?

1) Out of a maximum possible 384 pixels, 16 channels are open. When measured at the connector between the detector core and the JFET drawers, which ignores any problems in the JFET drawers, there are 12 open bolometers. Of these, 5 pixels were known to be missing or mechanically defective prior to their inclusion in the array. The remaining 4 defective channels have open circuits in the JFET drawers. While developing the JFET drawer assembly procedure, a large crack was made in one of the cold boards, severing a third of its traces. Most of these were salvaged with wirebonds and conductive epoxy, but two were not repairable and remained open. The other two JFET drawer open channels have open load resistors.

Additionally, 10 channel pairs and 1 channel triple are resistively shorted together (~ 1.5 MOhm), probably due to ionic contamination of the ceramic fanout boards during the connector soldering. There was 1 channel pair with a hard short in the JFET drawers.

2) To measure the heating of the bolometer frames by the nearby JFETs, the frame temperature was compared with the JFET heaters switched off and on. The temperature went from 366mK to 371 mK, a difference of 5 mK. This was considered acceptable. Additionally, the temperature drop along the conduction path from the PUD frames to the refrigerator was 12 mK with the JFET heaters switched on. These temperatures correlated well with predictions, and validated all of the choices in conductive glues and plating thicknesses for the thermal path from the bolometers to the refrigerator.

3) To measure the heating of the bolometer absorbers by the JFET Warm Board heaters, all the JFETs could not be switched off, because the bolometer signal could then not be read out. Instead, one of the JFET Warm Board heater temperature set points was varied, and the effect on the absorber temperature was measured. Comparing the dark IV curves with all three JFET boards heated to 120 K vs. one JFET board heated to 75 K, 4 pW additional power was seen on the operating bolometers at the higher temperature. The observed dark NEP of 1×10^{-16} W/(Hz)^{1/2} agrees with the prediction for a bolometer with this radiation. This attenuation of the JFET Warm Board radiation was considered acceptable.

4) With all three JFETs powered up, the temperatures of the load resistor boards are between 6.2 -7.2 K, so the heat sinking and isothermalization of the Cold Board was acceptable from that standpoint as well.

5) A rough indication of the instrument's microphonic susceptibility was obtained by rapping on the vacuum shell while the instrument was operating. An increase in the 100 Hz frequency component of the signal was seen, which was attributed to the fundamental mode of the entire detector rocking on its flexures. Other than that, vibrations of the detector signal chain had no measurable impact. During observations at the CSO, the telescope's motion did not affect the signal.

6) Finally, the additional power required to heat the JFETs to their operational temperature is 25-30 mW per drawer, and the dewar hold time, with the JFET warm boards at their operating temperature, exceeds 50 hours.

In summary, the thermal performance of the detector exceeds the requirements in all areas.

4. REFERENCES

1. D. A. Harper et al., "HAWC – a far-infrared camera for SOFIA", Proceedings Of SPIE, Vol. 4014, pp. 43-53, 2000
2. C. D. Dowell et al., "SHARC II: a Caltech submillimeter observatory facility camera with 384 pixels" in Astronomical Telescopes & Instrumentation: Millimeter and Submillimeter Detectors for Astronomy, Thomas G. Phillips, Jonas Zmuidzinas, Editors, Proceedings of SPIE Vol. 4855, pp. 73-87, 2003

3. S.H. Moseley et al., "Large-format bolometer arrays for far-infrared and submillimeter astronomy" in *Astronomical Telescopes & Instrumentation: Millimeter and Submillimeter Detectors for Astronomy*, Thomas G. Phillips, Jonas Zmuidzinas, Editors, Proceedings of SPIE Vol. 4805 (to be published 2002)
4. M. J. Li, C.A. Allen, S.A. Gordon, J.L. Kuhn, D.B. Mott, C.K. Stahle, L. L. Wang, "Fabrication of Pop-Up Detector Arrays on Si Wafers", Proceedings Of SPIE Vol. 3874 pp. 442-431, 1999
5. Epon 815 resin: Resolution Performance Products, Houston, TX 77251
Versamid 140 hardener: Cognis Chemicals, Kankakee, IL, 60901
6. C.A. Allen, S.H. Moseley, D.S. Schwinger, D.E. Franz, "Low Thermal Conductance Silicon Microwires Fabricated by MEMS Processing for Cryogenic Electrical Interconnects", *Nanospace 1998*, Houston, TX
7. High Density Printed Circuit Connector, Delphi Connection Systems, Irvine CA, 92614
8. J.G. Hust, "Low-temperature thermal conductivity of two fibre-epoxy composites", *Cryogenics* (1975) 15 126 – 128
9. Kevlar® Aramid Fiber Technical Guide, Dupont publication
10. Stycast 2850FT catalyst 24LV: Emerson & Cumming, Billerica, MA 01821
11. J.J. Bock, "Rocket-borne observation of singly ionized carbon 158 micron emission from the diffuse interstellar medium", PhD Dissertation, California Univ. Berkeley, CA, 1994, Physics dept, page 110